

19. PALEOGENE PYROCLASTIC VOLCANISM IN THE SOUTHWEST ROCKALL PLATEAU¹

Andrew C. Morton, British Geological Survey, Keyworth
and
John B. Keene, University of Sydney²

ABSTRACT

Three phases of volcanism have been recognized in the lower Paleogene sequence of the southwest Rockall Plateau which are related to the onset of seafloor spreading in the NE Atlantic. The earliest, Phase 1, is marked by a sequence of tholeiitic basalts and hyaloclastites which form the dipping reflector sequence in Edoras Basin. Phase 2 is characterized by tuffs and lapilli tuffs of air-fall origin, ranging in composition from basic to intermediate. They were generated by highly explosive igneous activity due to magma-water interaction, and terminate at the level of a major transgression. Subsequently, volcanism reverted to tholeiitic basalt type, producing the thin tuffs and minor basalt flows of Phase 3.

Alteration of the volcanic glass and diagenesis of the tuffs and lapilli tuffs has been considerable in many cases, with a large number of diagenetic mineral phases observed, including smectite, celadonite, analcime, phillipsite, clinoptilolite, mordenite, and calcite. Although calcite is the latest observed diagenetic cement, it nevertheless occurred relatively early, in one case totally preserving basaltic glass from alteration.

INTRODUCTION

Drilling in the southwest Rockall Plateau area during Legs 48 and 81 of the Deep Sea Drilling Project (DSDP) has shown that the area was the locus of substantial igneous activity during the early Paleogene. This extensive phase of basalt extrusion and associated pyroclastic volcanism took place in response to the separation of Rockall and Greenland. This chapter deals principally with the pyroclastic deposits recovered from Sites 552, 553, and 555 of Leg 81, supplementing the work of Harrison et al. (1979) on the Leg 48 material.

The petrographic characteristics of the tuffs and tuffaceous sediments were largely deduced through thin-section study, but several samples were examined with an ISI 60a scanning electron microscope (SEM), and the composition of feldspars and fresh and altered volcanic glasses was determined by electron microprobe, using an energy-dispersive X-ray analyzer. In view of the systematic X-ray diffraction (XRD) analyses of Leg 81 cores (Latouche and Maillet, this volume) and the detailed investigation into the nature of the secondary clay minerals associated with the basalts and tuffs (Desprairies, et al., this volume), only selected samples were analyzed by XRD.

The terminology adopted here follows the recommendations of Schmid (1981) regarding grain size and composition of pyroclastic deposits.

STRATIGRAPHIC DISTRIBUTION

Pyroclastic deposits encountered during Legs 48 and 81 (Fig. 1) in the Rockall Plateau area range in age from

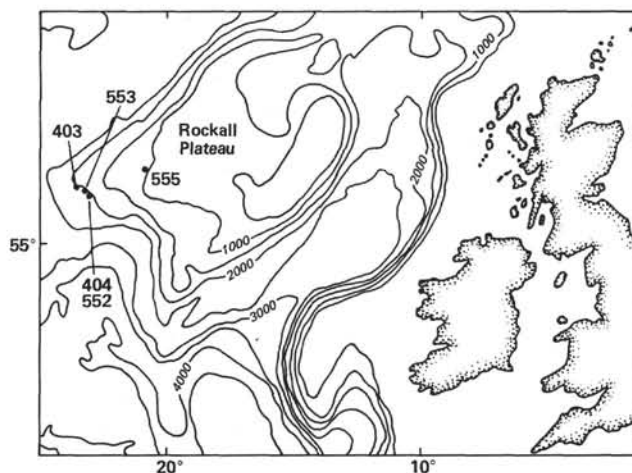


Figure 1. Location map of Rockall Plateau, with the Leg 48 and 81 sites mentioned in the text.

late Paleocene (NP9) to middle Eocene (NP16). The lower part of this sequence lies on basalt at Site 553 and is interbedded with basalt at Site 555. Thin basalts also occur in the higher parts of the succession, as exemplified by the flow recovered at the base of Hole 552. Although the top of the lower Paleogene sequence is marked by a hiatus at all sites, the upward decrease in abundance and thickness of tephra layers in the Eocene sediments suggests that the amount and intensity of pyroclastic volcanism has already begun to wane.

In detail, three phases of volcanism may be discerned (Table 1). The earliest, Phase 1, was reached at Sites 553 and 555 and is principally characterized by the basalts which form the dipping reflector sequence or its stratigraphical equivalents. However, pyroclastic deposits occur in association with the basalts, particularly at Site 555, where individual units of lapilli tuff and lapilli-tuff

¹ Roberts, D. G., Schnitker, D., et al., *Init. Repts. DSDP 81*: Washington (U.S. Govt. Printing Office).

² Addresses: (Morton) British Geological Survey, Keyworth, Nottingham NG12 5GG, United Kingdom; (Keene) Department of Geology and Geophysics, University of Sydney, Sydney, New South Wales 2006, Australia.

Table 1. Stratigraphic breakdown of lower Paleogene sequences of the Southwest Rockall Plateau into volcanic phases (defined in text).

	Hole 403	Hole 404	Hole 552	Hole 553A	Hole 555
Phase 3	26-3, 88 cm to 29-3, 116 cm (236.4-265.2 m)	7 to 17, CC (199.0-303.4 m)	8-4, 35 cm to 25 (T.D.) (160.3-314.0 m)	9-6, 30 cm to 12-4, 115 cm (234.8-261.1 m)	27 to 34-4, 22 cm (281.0-352.2 m)
Subphase 2b	29-3, 116 cm to 30, CC (265.2-280.0 m)	Absent		12-4, 115 cm to 14-1, 12 cm (261.1-274.6 m)	Absent (present in burrow fills 34-4, 22-32 cm?) (352.2-352.3 m)
Subphase 2a	31 to 46, CC (280.0-432.0 m)	18 to 26 (T.D.) (303.5-389.0 m)		14-1, 12 cm to 26-1, 20 cm (274.6-388.7 m)	34-4, 22 cm to 48, CC (352.2-490.0 m)
Quiescent phase	47 to 52 (T.D.) (432.0-489.0 m)			26-1, 20 cm to 34-1, 13 cm (388.7-464.6 m)	49 to 62-5, 5 cm (490.0-619.5 m)
Phase 1				34-1, 13 cm to 59 (T.D.) (464.6-682.5 m)	62-5, 5 cm to 783 (619.5-822.5 m)

agglomerate reach some 40 m in thickness. These thick, coarse pyroclastics are intimately associated with pillow basalts and undoubtedly represent the products of brecciation of basalt flows in a submarine environment. The numerous thinner tuffs and lapilli tuffs also present in the Phase 1 sequence are similarly interpreted as hyaloclastite, for a number of reasons. First, they resemble the thicker units on compositional grounds, in that the volcanoclasts are exclusively basaltic. Second, both contain the secondary zeolite analcime, suggesting relatively high-temperature alteration, which is inconsistent with an air-fall origin. Finally, individual tuff beds rarely show the fining-upward characteristics of air-fall tuffs; in most cases, the beds are ungraded and chaotic, and some even show upward coarsening (e.g., 555-85-1, 85 cm to 85-2, 50 cm). At Site 555 hyaloclastites and basalts dominate the sequence down to Core 83. Below this level and above the dolerite recorded at T.D. only minor basalts and lapilli tuffs are present in a mainly clastic sequence of late Paleocene (NP9) age. The high temperature alteration of the dolerite (Harrison and Merriman, this volume) indicates that it is probably intrusive. Therefore the record of extrusive volcanism is meager below Core 83, suggesting that the base of the hyaloclastite-basalt unit marks the onset of the major extrusive event which led to the formation of the basaltic dipping reflector sequence in Edoras Basin. If this is so, it implies that this event occurred in the latest Paleocene.

A time of relative quiescence followed, with little or no evidence for pyroclastic activity in a period of accumulation of terrigenous clastics in marginal marine or estuarine conditions. This quiescent period has been noted at Holes 403, 553A, and 555 and may also have been reached in Hole 404. The absence of pyroclastic deposits is not the result of nonpreservation because of unfavorable depositional conditions, because mudstone (with high preservation potential for tuff horizons) predominates at Site 555, although the interval at most sites is dominated by sandstone.

The sudden reappearance of frequent beds of tuff and lapilli tuff (Table 1, Fig. 2) marks the onset of Phase 2

volcanism. The lowermost Phase 2 tuffs occur in sediment barren of calcareous nannofossils, but forms indicative of the lower part of NP10 appear close to the base of the sequence (Backman, this volume). The glauconitic level which marks the end of Phase 2 activity also lies within NP10 close to the NP10/11 boundary; Phase 2 activity is therefore confined to this zone.

The phase may be subdivided into a lower unit, 2a, and an upper unit, 2b. Subphase 2a occurs at all sites except 552, which did not penetrate Phase 2 volcanics, and is characterized by relatively thin beds of tuff and lapilli tuff, with maximum clast diameters reaching 3 cm at most sites. Apart from a considerable number of tuffs disturbed by bioturbation and reworking, most show upward fining, consistent with an air-fall derivation. Thirty-six tuff and lapilli tuff beds occur at Site 553, a number similar to that at the adjacent Site 403 (34 noted here). Fewer are recorded at 404 (nine only), but recovery at this site was very poor; it is also possible that the base of the Phase 2 sequence was not penetrated. There are also fewer beds at Site 555 (26 in all), but the relatively good core recovery over the interval indicates that this is a genuine reduction in numbers. There is little obvious difference in depositional environment between this site and the others, but it is conceivable that more tuff horizons have been destroyed through reworking and bioturbation than elsewhere.

Subphase 2b is only recorded at Sites 403 and 553, and represents a considerable quantity of pyroclastic debris. In both holes, it occurs as a single unit of highly reworked and bioturbated lapilli tuff, some 15 m thick at Site 403 and 13.5 m thick at Site 553; maximum clast diameters approach 2 cm. A particularly characteristic feature of this lapilli tuff is that it possesses a matrix of blue-green celadonite.

The top of Phase 2 is marked by a change to highly glauconitic sediment. Although the glauconitic horizon occurs at all sites (excluding 552), the underlying Subphase 2b volcanics are absent at Sites 404 and 555. However, at Site 555 large cylindrical burrows (diameter 2.5 cm) occur immediately below the disconformity (Sam-

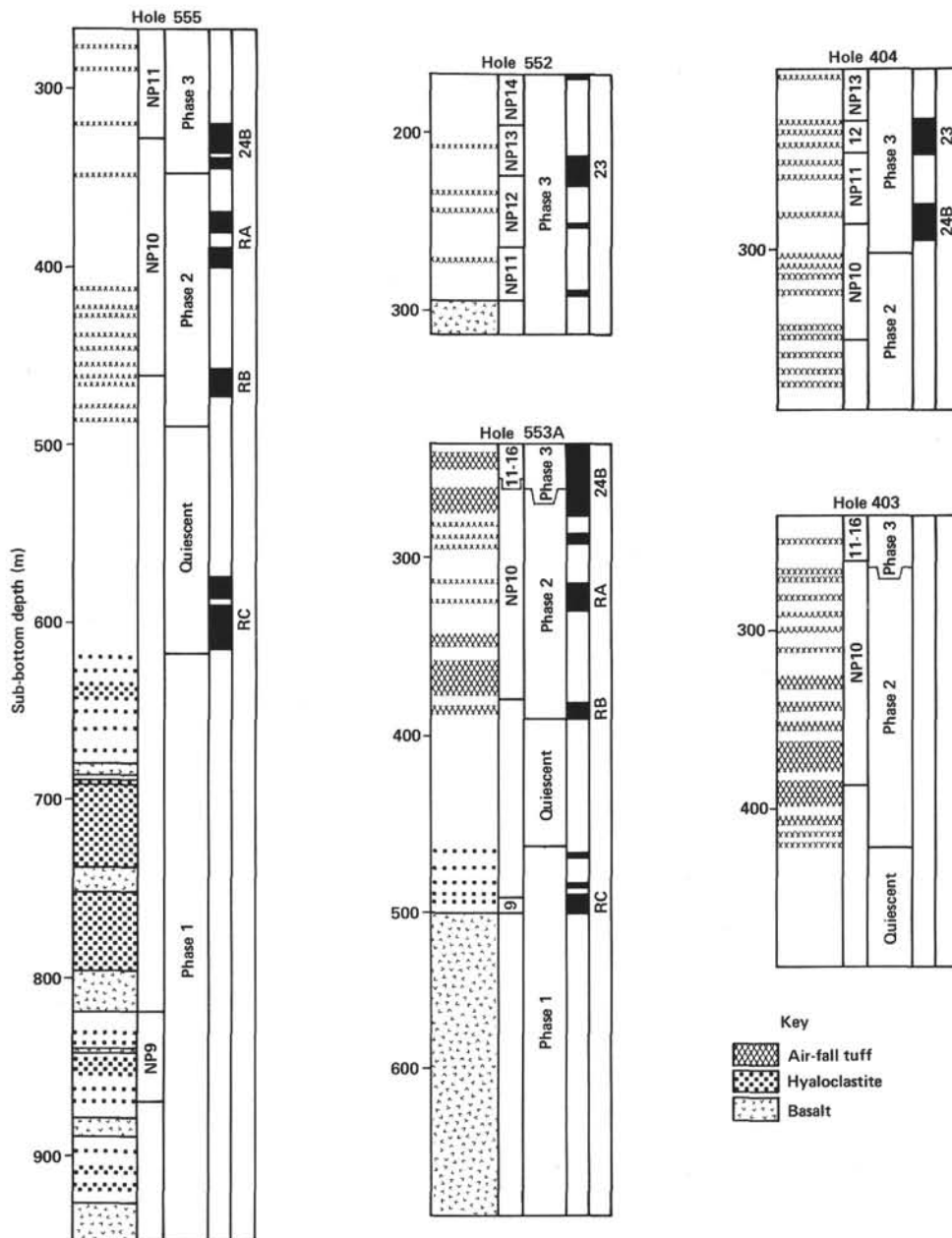


Figure 2. Schematic representation of the distribution of pyroclastic and basaltic rocks in the lower Paleogene sites of the SW Rockall Plateau, and their relationship to the nannoplankton zonation and magnetic reversals.

ple 555-34-4, 22–32 cm). These burrows are infilled with coarse lapilli tuff, a lithology not recorded *in situ* at this level or immediately adjacent, the closest lapilli tuff being found in Core 39 (Sample 39-1, 77–104 cm). They may therefore be the only record of the Subphase 2b activity at Site 555.

The tuffs which occur above the base of the glauconitic datum comprise Phase 3. They are, in general, much finer grained, thinner, and less frequent than those of Phase 2; in total, at all Leg 48 and 81 sites under consideration, 20 tuff beds occur. Of these, nine occur in NP11, eight in NP12, two in NP13, and one in NP16. There is also a marked change in composition compared

to the Phase 2 tuffs, as will be discussed later. Clearly the Phase 2–Phase 3 transition represents a sudden decline in intensity of pyroclastic volcanism, which then appears to have further waned throughout the early and middle Eocene.

MINERALOGY AND CHEMISTRY

Phase 1

Phase 1 pyroclastic deposits are dominantly composed of lapilli-sized volcanoclasts. Vitric components predominate, although feldspar–microlitic lithic particles are common in a small number of samples. Vesicularity of the

glass is highly variable between samples, but where present, vesicles tend to be spheroidal. The volcanic glass is exclusively of tholeiitic basalt type (Table 2, Fig. 3), typically with low K_2O contents. Hydration and alteration to smectite has occurred to some extent in all cases.

Crystal components, in the form of plagioclase phenocrysts, are consistently present in minor amounts (Plate 1, Fig. 1). They are particularly characteristic, in that they are commonly very large (up to 4 mm), and many are al-

tered to smectite and analcime. Unzoned, unaltered grains vary from An_{68} to An_{74} (calcic labradorite to bytownite); zoned crystals have calcic bytownite cores (up to An_{85}) and more sodic margins (down to An_{73}) (Fig. 4).

Phase 2

Phase 2 pyroclastics are considerably more variable in composition than are those of Phase 1. In general, however, lithic components are more common than in

Table 2. Chemical analyses of volcanic glass from the Leg 81 Paleocene-Eocene pyroclastic deposits by electron microprobe.

Oxide	Phase 1		Subphase 2a			Subphase 2b		Phase 3		
	555-85-2, 38-40 cm	555-67-1, 56-58 cm	555-43-4, 129-131 cm	555-42-1, 31-33 cm	553A-25-2, 83-85 cm	554A-14-4, 60-62 cm	553A-13-1, 82-85 cm	555-27-1, 27-28 cm	553A-11-3, 97-98 cm	552-12-2, 106-108 cm
SiO ₂	43.1	36.8	56.5	47.3	48.8	54.2	50.8	47.6	48.0	48.2
Al ₂ O ₃	9.9	12.3	13.5	15.6	11.5	19.1	8.6	12.0	14.1	14.6
TiO ₂	0.6	1.9	1.2	2.8	0.1	0.3	0.3	3.7	2.6	2.3
Cr ₂ O ₃	0.0	0.0	0.0	0.0	0.0	0.0	0.0	0.1	0.0	0.2
FeO*	19.6	22.2	14.4	14.5	13.9	1.6	16.8	17.2	13.5	13.3
MgO	14.5	14.9	4.6	5.5	12.1	0.1	12.0	5.4	7.1	7.1
MnO	0.2	0.9	0.0	0.4	0.0	0.1	0.0	0.4	0.3	0.1
CaO	2.1	0.8	0.3	8.8	0.9	4.6	0.4	9.7	10.8	10.6
Na ₂ O	2.4	1.5	1.3	4.4	2.5	3.5	2.6	3.0	2.9	3.1
K ₂ O	0.2	0.2	1.0	0.5	0.4	5.6	0.8	0.3	0.2	0.2
Total	92.6	91.5	92.8	99.9	90.2	89.1	90.3	99.8	99.5	99.7

Note: FeO* = all iron calculated as FeO.

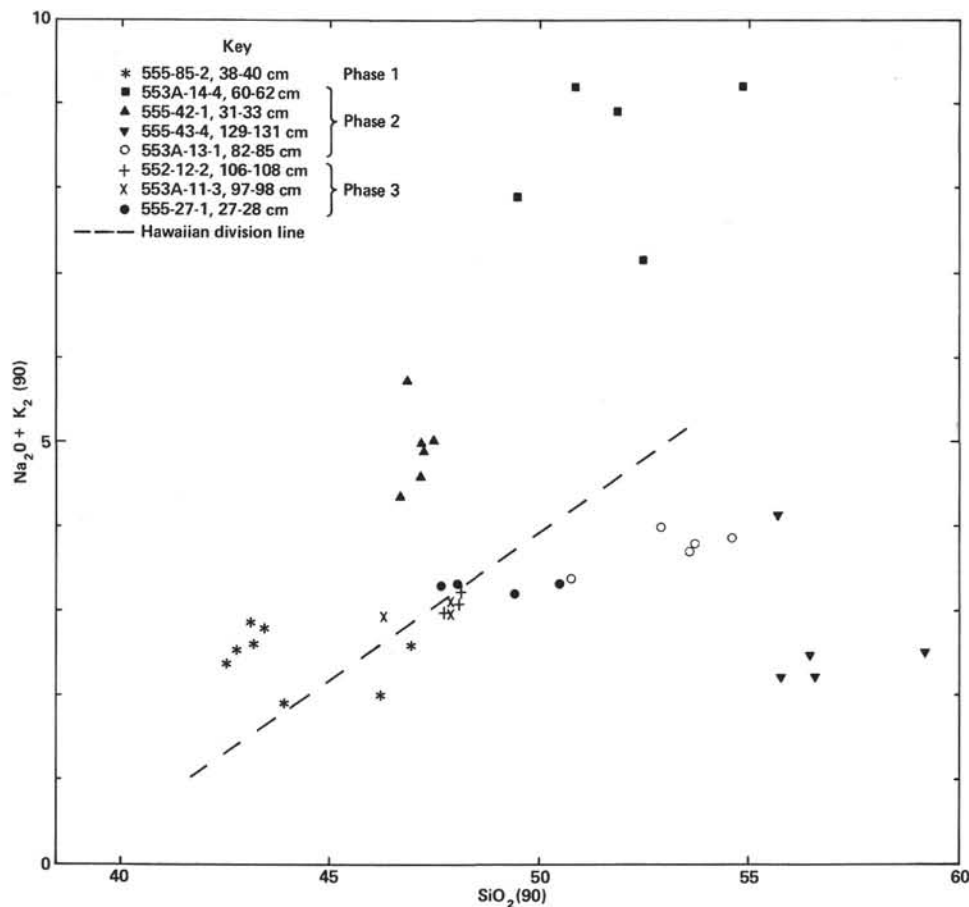


Figure 3. Alkalis-silica plot of typical volcanic glasses from the Leg 81 pyroclastic deposits. Hawaiian division line taken from MacDonald and Katsura (1964). Note the tendency for originally tholeiitic glasses (Phase 1) to cross the Hawaiian division line during the alteration process, principally through silica loss. Note the extreme alkali enrichment in the Phase 2 glass from Sample 553A-14-4, 60-62 cm.

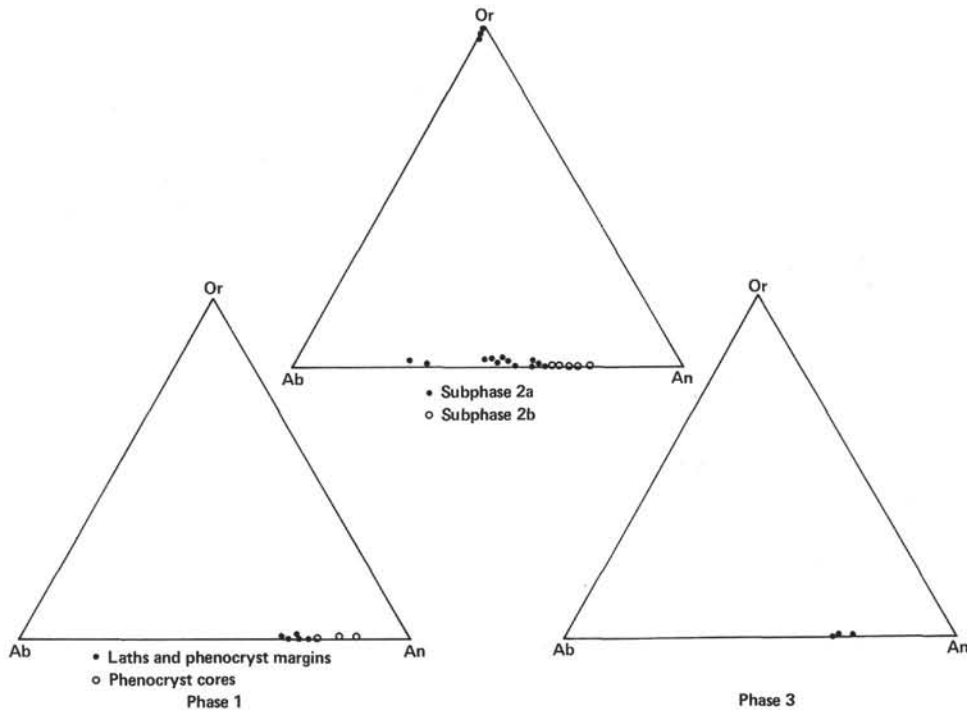


Figure 4. Compositions of feldspars of pyroclastic origin in the lower Paleogene sediments of Leg 81.

Phase 1, although vitric material still predominates. As with Phase 1 material, alteration of volcanic glass has occurred in most cases, but one sample (555-42-1, 31–33 cm) has been protected from alteration by very early diagenetic calcite cementation. The glass in this sample is considerably richer in alkalis than those of either Phase 1 or 3 (Table 2), being of alkali-basalt composition. It contains nepheline in the norm (Table 3) and lies above the Hawaiian division line of MacDonald and Katsura (1964) (Fig. 3). The original chemistry of the other Phase 2 glasses is less easy to ascertain because of alteration, but in general they have similar SiO_2 contents to the basalts of Phase 1, although some are more siliceous. Although K_2O contents are higher, in one case abnormally so (Table 2), the magmas are still mainly tholeiitic. Some vitric

particles in the Subphase 2b tuff have been altered to chlorite, indicating high temperature alteration at source.

The compositional range of feldspars in the Phase 2 pyroclastics also reflects the more variable chemistry. Subphase 2a feldspars vary from andesine (An_{30}) to labradorite (An_{67}); those in 2b are more calcic (An_{65} – An_{77}) (Fig. 4B). Also present in some samples from Subphase 2a are virtually pure orthoclase pseudomorphs after plagioclase (Fig. 4). In one case (Sample 553A-14-4, 60–62 cm) potassium enrichment has also occurred in the accompanying glass (Table 2). This is presumably the result of potash metasomatism: the presence of unaltered pyroclastic and rounded detrital feldspars of oligoclase composition in coexistence with these sanidines suggests that the metasomatism took place prior to their incorporation into the sediment, i.e., at the site of eruption.

Table 3. CIPW-normative analyses of unaltered basaltic glass from Leg 81 pyroclastic deposits.

Mineral	Sample (interval in cm)			
	552-12-2, 106–108	553A-11-3, 97–98	555-27-1, 27–28	555-42-1, 31–33
Albite	25.9	24.0	25.9	26.7
Orthoclase	1.0	0.8	1.6	3.0
Anorthite	25.8	26.2	18.0	21.1
Nepheline	0.0	0.0	0.0	5.9
Diopside	22.1	22.1	25.1	18.8
Hypersthene	4.1	8.4	13.6	0.0
Olivine	13.5	10.5	5.3	16.0
Magnetite	3.0	3.0	3.8	3.2
Ilmenite	4.4	4.9	6.7	5.3
Chromite	0.2	0.1	0.0	0.0

Note: $\text{Fe}_2\text{O}_3/\text{FeO}$ taken as 0.15 (Brooks, 1976).

Phase 3

The Phase 3 tuffs are dominated by vitric material, with lithic and crystal components making up a very minor part of the pyroclastic contribution. The glass is rarely altered because of the increased SiO_2 content in the pore waters resulting from the abundance of siliceous microfossils in the associated sediment. The glass is exclusively of the tholeiitic basalt type (Tables 2 and 3, Fig. 3), and shows little variation between sites, although those at Site 555 have slightly higher Fe/Mg ratios than those from Sites 552 and 553. TiO_2 contents are higher than those of the underlying basalts and tuffs. Although plagioclase is the most abundant member of the associated crystal fraction, grains are not common. The few grains analyzed reflect the exclusively basaltic sources (An_{68} to An_{74} , Fig. 4). Augite also occurs as a phenocryst phase

is several samples, and iddingsite has been found in one case (Sample 552-19,CC).

ALTERATION AND DIAGENESIS

Authigenic and Syngenetic Components

The postdepositional phases present in the tuffaceous sediments of Sites 552, 553, and 555 include smectite, celadonite, clinoptilolite, phillipsite, mordenite, analcime, calcite, pyrite, and cristobalite. In addition, syngenetic glauconite pellets and oolites are common at certain horizons.

Authigenic smectite is confined to Phases 1 and 2. It forms rims around framework grains (detrital and biogenic particles as well as pyroclasts), infills vesicles, and partially replaces some pyroclastic feldspars (Plate 1, Fig. 1). Under the SEM (Plate 1, Fig. 2) it shows the characteristic honeycomb texture figured by Wilson and Pittman (1977). XRD analysis shows the smectite to be saponite (Merriman, pers. comm., Desprairies et al., this volume).

Authigenic needles of blue-green celadonite (Plate 1, Fig. 3) occur throughout the thick lapilli tuff unit which composes Subphase 2b at Site 553 (e.g., Samples 553A-12-5, 30–32 cm and 553A-13-1, 82–85 cm), and in the stratigraphically equivalent unit at Site 403 (Harrison et al., 1979). As with smectite, celadonite fringes all framework grains and even occurs as a cavity-fill to gastropod shells. It also occurs as a replacement of the groundmass of lithic pyroclasts. Celadonite is also present in the Phase 3 sequence, having been detected in the groundmass of a number of samples (Samples 553A-11-4, 77–78 cm; 552-13-1, 86–88 cm; and 404-16,CC).

Four types of zeolite have been recognized in this study: clinoptilolite, phillipsite, mordenite, and analcime. Of these, clinoptilolite occurs throughout the sequence and is not, apparently, necessarily related to volcanic input, being present both in tuffaceous and nontuffaceous samples (Plate 1, Fig. 4). Phillipsite has only been recorded from Phase 2 tuffs, both at Site 553 (e.g., Sample 553A-14-4, 60–62 cm) and at Site 555 (e.g., Sample 555-46-2, 66–70 cm). Both in thin section (Plate 2, Fig. 1) and under the SEM (Plate 2, Fig. 2) it shows a radiating habit, similar to that figured by Pevear et al. (1982). Its presence in the Phase 2 sequence and absence from Phases 1 and 3 suggests that the composition of the pyroclasts was a major control on its genesis. The glasses of Phase 2 are generally richer in potassium than are those of the underlying and overlying phases (Table 2), particularly where potash metasomatism has taken place. The release of potassium during alteration appears to have promoted the generation of the potassium-bearing zeolite, phillipsite.

Mordenite occurs in one sample only (552-19,CC), where it is the major phase, virtually wholly replacing the pre-existing volcanic glass. SEM investigation shows it to have a typical fibrous habit (Plate 2, Fig. 3).

Analcime is confined to the Phase 1 pyroclastics. As with the other zeolites, it clearly developed after the generation of smectite, but prior to calcite cementation (Plate 2, Fig. 4). As discussed by Hay (1966), analcime is thought to occur through replacement of pre-existing zeolites

under slightly elevated temperatures and pressures, a view consistent with the appearance of analcime well below the top of the lava pile in Iceland, for example (Walker, 1960). However, in this case several facts argue against a burial depth generation of analcime from a zeolite precursor. The first appearance of analcime is at 34-1, 70–75 cm in Hole 553A, about 465 m sub-bottom, much shallower than at Site 555, where it appears in Sample 64-5, 23–25 cm, a burial depth of some 640 m. As will be discussed, although calcite cementation took place after analcime (Plate 2, Fig. 4), it occurred sufficiently early in diagenesis to prevent substantial alteration of volcanic glass, and, hence, before significant burial had taken place. This neither allows much time for the generation of a precursor zeolite, nor produces sufficient temperature elevation to effect the transformation. Thirdly, no evidence for a precursor zeolite can be found in the analcime texture. Finally, nonvolcanogenic sediment interbedded with analcime-cemented lapilli tuffs contains clinoptilolite (e.g., Sample 555-69-5, 95–98 cm). This is inconsistent with an origin by depth-controlled zeolite transformation.

The occurrence of an early diagenetic, relatively high-temperature phase in these tuffs and its absence in the interbedded nonvolcanogenic but zeolite-bearing sediment suggests that the pyroclastic material itself provided the necessary heat. On this basis it appears likely that the Phase 1 pyroclastics were at relatively high temperatures at the time of deposition, precluding an air-fall origin. This, and their association with major basalt extrusion, clearly indicates a hyaloclastite origin for these deposits.

Coarse sparry calcite commonly cements the tuffs and lapilli tuffs of Phases 1 and 2, infilling vesicles and replacing many pre-existing grains, particularly mica and feldspar. Although calcite cementation is the latest major diagenetic phase to have occurred, post-dating smectite and zeolite (Plate 2, Figs. 1, 4), it nevertheless preserves volcanic glass from substantial alteration; indeed, in one case (Sample 555-42-1, 31–33 cm), cementation was so early that no alteration is apparent. The common association of calcite cement with tuff horizons is probably the result of release of considerable amounts of calcium during alteration of volcanic glass.

Minor diagenetic phases include pyrite and disordered cristobalite. Pyrite octahedra mainly occur in samples containing a detrital carbonaceous clay matrix and probably formed early in diagenesis under reducing conditions. Pyrite also occurs as a replacement of siliceous microfossil tests in association with glauconite. Cristobalite occurs as a cement in some Phase 3 tuffs (e.g., 555-30,CC).

Glauconitic material is present in several samples from all three sites examined. It is particularly common at the junction between Phases 2 and 3 (e.g., Samples 553A-12-3, 30–32 cm and 555-34-2, 110–112 cm). The mineralogy, chemistry, and mode of occurrence of this material is discussed more fully elsewhere (Morton et al., this volume). As pointed out by Harrison et al. (1979) glauconite occurrence is essentially unrelated to the pyroclast content, since it is present in both tuffaceous and non-

tuffaceous samples. However, in one tuff (Sample 553A-12-5, 30–32 cm and 12,CC [5–7 cm]) the volcanic glass is altered to a mineral rich in potassium (Table 4) which optically resembles glauconite. However, XRD analysis proves this to be iron-rich smectite (Merriman, pers. comm.).

Alteration of Volcanic Glass

As already noted, the volcanic glasses belonging to Phases 1 and 2 have suffered variable degrees of alteration. Petrographically, minor alteration is manifested by the development of a wavy birefringence; more altered glass has acquired the speckly birefringence characteristic of smectite.

Investigations into the chemistry of the glass and altered glass by electron microprobe reveal that trends of element enrichment and depletion occurred during the alteration process. In addition, there appear to have been two different types of alteration, presumably a function of the chemistry of the interacting components. These trends are illustrated here by considering the effects of alteration on seven major elements (Si, Al, Fe, Mg, Ca, Na, and K) in a number of samples (Table 4).

Considering first the Phase 1 basaltic glass (Sample 555-85-2, 38–40 cm), and assuming primary similarity with the average composition of Site 555 basalts (Harrison and Merriman, this volume), it can be seen that Si, Al, and particularly Ca have been lost, Fe and Mg have been enriched, and Na and K show no discernible trend—in the case of the latter because of its very low initial concentration. A variably altered basaltic glass from Phase 2 at Site 555 (Sample 555-40-6, 49–51 cm) shows a similar trend, with loss of Si, Al, Ca, Na, and K and gain of Fe and Mg. The metasomatized glass (Sample 553A-14-4, 60–62 cm) also shows loss of Si, Al, Ca, Na, and K on alteration; again, Fe and Mg are enriched.

These three examples are typical of the alteration of volcanic glasses in the Leg 81 material—the virtual disappearance of Ca, the loss of Si, Al, Na, and K, and the relative gain in Fe and Mg. However, the samples from 553A-12,CC (5–7 cm) and 553A-13-1, 82–85 cm show a different trend. They are taken from near the top and bottom, respectively, of the Subphase 2b tuff which immediately underlies the glauconitic datum level at the site. The glass at the base of the tuff shows weak wavy

birefringence and is clearly less altered than the material at the top, which petrographically resembles glauconite, although XRD analysis proves it to be iron-rich smectite. In this case, Ca, Si, Al, Mg, and Na have been lost from the glass, whereas Fe and K are relatively enriched. This tuff, therefore, shows a distinctly different alteration trend, with Mg (normally enriched) having been leached, and K (normally leached) having been enriched (Table 3). As such, it is the only Leg 81 tuff to show the alteration trends typical of basalts interacting with seawater at low temperatures (Hart, 1970; Thompson, 1973; Table 5).

The fundamental difference between the Subphase 2b lapilli tuff and those underlying it is that it lies immediately below the glauconitic datum level which marks a major marine transgression over the area. As such, it is the only pyroclastic deposit to have interacted with seawater of normal salinity: the underlying tuffs were, in general, deposited in poorly oxygenated nearshore or estuarine conditions (see site chapters and Murray, this volume). Moreover, the Subphase 2b tuff was exposed to seawater for a long period; the high concentration of glauconite in the overlying level is an indication of very low sedimentation rates at this time. The underlying pyroclastics were rapidly buried and consequently did not interact with fluids at the sediment–water interface for extended periods. The differences in alteration trends no doubt reflect these factors.

ORIGIN OF THE PYROCLASTIC DEPOSITS

Two alternative mechanisms have been proposed for the generation of dipping reflector sequences. Roberts et al. (1979) suggested that the SW Rockall Plateau dipping reflectors represent a sequence of lavas, pyroclastic and sediments deposited on thinned continental crust immediately prior to the onset of seafloor spreading; Hinz (1981) has ascribed a similar origin to other seaward-dipping wedges on passive margins. However, Talwani et al. (1981), Mutter et al. (1982), and Smythe (1983) have suggested that they represent oceanic crust created by seafloor spreading, with accretion occurring subaerially.

The former hypothesis, that the dipping reflector sequence represents the rifting phase and that the onset of seafloor spreading is marked in the SW Rockall Plateau

Table 4. Alteration of volcanic glass as shown by electron microprobe analysis. (Average basalt taken from Harrison and Merriman, this volume.)

Oxide	Site 555 Average basalt (unaltered)	Sample 555-85-2, 38–40 cm	Sample 555-40-6, 49–51 cm		Sample 553A-14-4, 60–62 cm		Sample 553A-13-1, 82–85 cm	Sample 553A-12-CC, 5–7 cm
		Highly altered glass	Altered glass	Highly altered glass	Altered glass	Highly altered glass	Altered glass	Highly altered glass
SiO ₂	49.7	42.0	50.9	27.3	52.5	36.6	50.8	48.3
Al ₂ O ₃	13.8	8.5	20.1	10.5	19.5	6.6	8.6	4.7
TiO ₂	1.3	1.3	3.6	0.0	0.1	0.1	0.3	0.3
FeO*	11.6	18.0	8.5	30.7	4.3	16.6	16.8	23.9
MgO	7.1	14.2	2.9	6.5	2.4	11.4	12.0	3.4
CaO	12.1	2.5	0.4	0.4	6.2	0.2	0.4	0.3
Na ₂ O	2.3	2.4	1.8	1.0	3.3	2.6	2.6	1.1
K ₂ O	0.1	0.1	0.8	0.0	4.0	1.1	0.8	6.7
Total	98.0	89.0	89.0	76.4	92.2	75.2	90.3	88.7

Note: FeO* = all iron calculated as FeO.

Table 5. Trends of element enrichment and depletion in the alteration of volcanic glass from the Leg 81 sequences compared to alteration trends of ocean-floor basalt.

Oxide	Samples		Alteration of basalt (Hart, 1970)	Alteration of basalt (Thompson, 1973)
	553A-14-4, 60-62 cm 555-40-6, 49-51 cm 555-82-4, 38-40 cm	553A-12, CC (5-7 cm) 553A-13-1, 82-85 cm		
SiO ₂	Loss	Loss	Loss	Loss
Al ₂ O ₃	Loss	Loss	Unchanged	Variable
FeO	Gain	Gain	Gain	Variable
MgO	Gain	Loss	Loss	Loss
CaO	Loss	Loss	Loss	Loss
Na ₂ O	Loss	Loss	Gain	Variable
K ₂ O	Loss	Gain	Gain	Variable

area by the change from Phase 2 to Phase 3 volcanism, is attractive in some respects, particularly regarding the genesis of the glauconitic horizon. Subsidence is a well-documented response to the onset of seafloor spreading (Sleep, 1971). Such subsidence in the SW Rockall Plateau area would cause an influx of fully marine waters over the existing nearshore or lagoonal areas, thus producing ideal conditions for glauconite genesis.

However, the hypothesis does not adequately explain the quiescent phase nor the change from extrusive to explosive volcanism (Phase 1-Phase 2 transition). Furthermore, the essentially oceanic nature of the basalts (Harrison and Merriman, this volume) and tephra recovered during Leg 81, and the absence of interbedded sediment in the part of the dipping reflector sequence drilled at Site 553 favor the "subaerial seafloor spreading" hypothesis. The patterns of pyroclastic activity also accord well with this model, and it explains the aspects mentioned above which are difficult to reconcile with the rifting model.

Volcanism began in late Paleocene times with subaerial extrusion of typical low-potassium oceanic tholeiites in Edoras Basin (Site 553). Away from the locus of volcanism, shallow marine conditions predominated (Site 555), so that as the basalts entered the submarine environment, pillow lavas and hyaloclastites developed. With continued extrusion, the drilled locations migrated eastward relative to the active ridge crest, explaining the diachronism of the cessation of Phase 1 volcanism between Sites 553 and 555 (Fig. 2). As subsidence and migration continued, Site 553 also became submerged so that lava emplacement ceased to be subaerial, with the consequent development of hyaloclastite. Further migration caused the total cessation of Phase 1 activity at the drilled locations, producing the observed quiescent phase. However, seismic profiles show continued development of dipping reflectors to the west at this time.

It is generally agreed that generation of basaltic air-fall pyroclastics requires water-magma interaction. Consequently, the onset of Phase 2 volcanism may be taken to mark the time when the active ridge crest began to subside below sea level. Such interaction is supported petrographically by the occurrence of chloritized volcanic particles and potash metasomatism, both indications for high-temperature interaction between magma and seawater. This is also supported by the similarity in magma composition between the Phase 1 and Phase 2 volcanics, both being tholeiitic in virtually all cases, with

the only exception being the alkali-basaltic tuff at Site 555.

The cessation of Phase 2 volcanism may similarly be taken to mark the point at which the ridge crest became wholly submerged. From this time onward, basalt flows were extruded underwater, so that their flow lengths became considerably shorter. As a consequence, lava build-up failed to occur as it had in the subaerial setting, and subsidence rates therefore began to greatly exceed rates of deposition. This led to rapid inundation of the area by the sea, which, coupled with the cut-off in supply of detrital material from Greenland (Morton, this volume), produced very slow sedimentation rates and an ideal environment for glauconite generation (Morton et al., this volume).

The thin tuffs recorded in the lower Paleogene sediments above the glauconitic level are of distinctly different composition from those of Phases 1 and 2. Although they are, nevertheless, tholeiitic, their TiO₂ contents are much higher. This indicates either a change in magma chemistry at this time or that the tuffs are more distally derived. The lower TiO₂ contents of the Site 554 basalt (Harrison and Merriman, this volume) and the fine grain size of the tuffs suggest that the latter may be the case. The basalts of East Greenland and the Faeroes are higher in TiO₂ than those of the SW Rockall Plateau (Brooks et al., 1976, Noe-Nygaard and Rasmussen, 1968) and are chemically similar to the Phase 3 tuffs, suggesting that their source may lie to the north.

ACKNOWLEDGMENTS

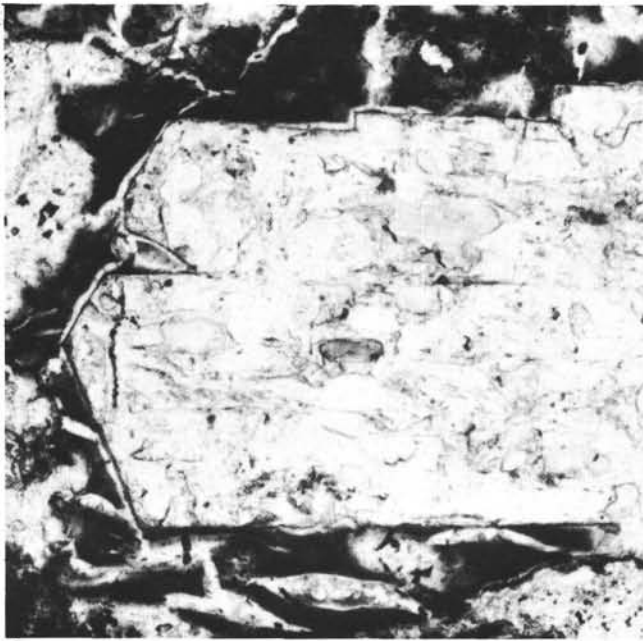
The authors wish to thank Dr. M. T. Styles and Mr. P. H. A. Nancarrow for their assistance with the electron microprobe, Mr. R. J. Merriman for XRD analysis, and Mr. R. I. Lawson for calculation of the CIPW norms. A. C. Morton is grateful to the U.K. Department of Energy for funding his participation in Leg 81. The contribution is published with the approval of the Director of the British Geological Survey (N.E.R.C.).

REFERENCES

- Brooks, C. K., 1976. The Fe₂O₃/FeO ratio of basalt analyses: An appeal for a standardized procedure. *Bull. Geol. Soc. Denmark*, 25: 117-120.
- Brooks, C. K., Nielsen, T. F. D., and Petersen, T. S., 1976. The Blossville Coast basalts of East Greenland: Their occurrence, composition and temporal variations. *Contrib. Mineral. Petrol.*, 58: 279-292.
- Harrison, R. K., Knox, R. W. O'B., and Morton, A. C., 1979. Petrography and mineralogy of volcanogenic sediments from DSDP Leg 48, southwest Rockall Plateau, Sites 403 and 404. In Montadert, L., Roberts, D. G. et al., *Init. Repts. DSDP*, 48: Washington (U.S. Govt. Printing Office), 771-785.
- Hart, R., 1970. Chemical exchange between seawater and deep ocean basalts. *Earth Planet. Sci. Lett.*, 9:269-279.
- Hay, R. L., 1966. Zeolites and zeolitic reactions in sedimentary rocks. *Geol. Soc. Am. Spec. Publ.*, 85.
- Hinz, K., 1981. A hypothesis on terrestrial catastrophes. Wedges of very thick oceanward dipping layers beneath passive continental margins—Their origin and palaeoenvironmental significance. *Geol. Jb.*, E22:3-38.
- MacDonald, C. A., and Katsura, T., 1964. Chemical composition of Hawaiian lavas. *J. Petrol.*, 5:82-133.
- Mutter, J. C., Talwani, M., and Stoffa, P. L., 1982. Origin of seaward-dipping reflectors in oceanic crust off the Norwegian margin by "subaerial sea-floor spreading." *Geology*, 10:353-357.
- Noe-Nygaard, A., and Rasmussen, J., 1968. Petrology of a 3000 metre sequence of basaltic lavas in the Faeroe Islands. *Lithos*, 1:286-304.

- Pevear, D. R., Dethier, D. P., and Frank, D., 1982. Clay minerals in the 1980 deposits from Mount St. Helens. *Clays Clay Mineral.*, 30:241-252.
- Roberts, D. G., Montadert, L., and Searle, R. C., 1979. The western Rockall Plateau: Stratigraphy and structural evolution. In Montadert, L., Roberts, D. G., et al., *Init. Repts. DSDP*, 48: Washington (U.S. Govt. Printing Office), 1061-1088.
- Schmid, R., 1981. Descriptive nomenclature and classification of pyroclastic deposits and fragments. *Geol. Rundschau*, 70:794-799.
- Sleep, N. H., 1971. Thermal effects of the formation of Atlantic continental margins by continental break-up. *Geophys. J. R. Astron. Soc.*, 24:325-350.
- Smythe, D. K., 1983. Faeroe-Shetland escarpment and continental margin north of the faeroes. In Bott, M. H. P., et al., (Eds.), *Structure and Development of the Greenland-Scotland Ridge—New Methods and Concepts*: London (Plenum Press), 109-119.
- Talwani, M., Mutter, J., and Eldholm, O., 1981. The initiation of opening of the Norwegian Sea. *Oceanologica Acta*, SP, pp. 23-30.
- Thompson, G., 1973. A geochemical study of the low temperature interaction of seawater and oceanic igneous rock. *EOS, Trans. Am. Geophys. Union*, 54:1015-1019.
- Walker, G. P. L., 1960. Zeolite zones and dyke distribution in relation to the structure of the basalts in eastern Iceland. *J. Geol.*, 68: 585-528.
- Wilson, M. D., and Pittman, E. D., 1977. Authigenic clays in sandstones: Recognition and influence on reservoir properties and paleoenvironmental analysis. *J. Sediment. Petrol.*, 47:3-31.

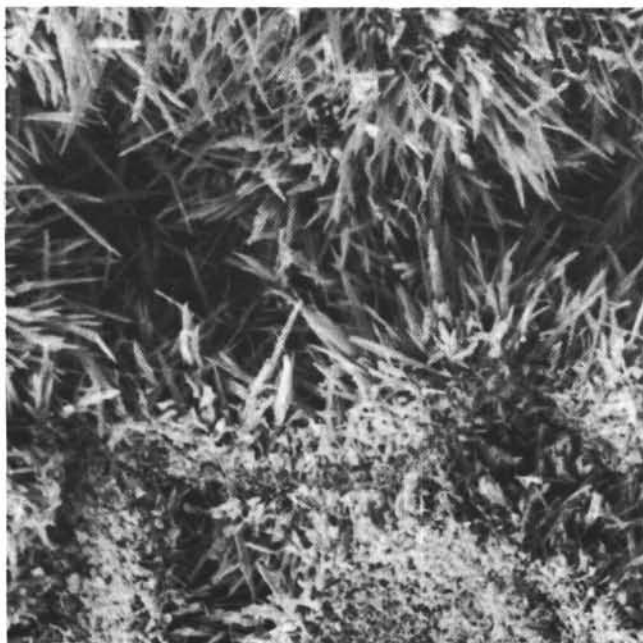
Date of Acceptance: June 24, 1983



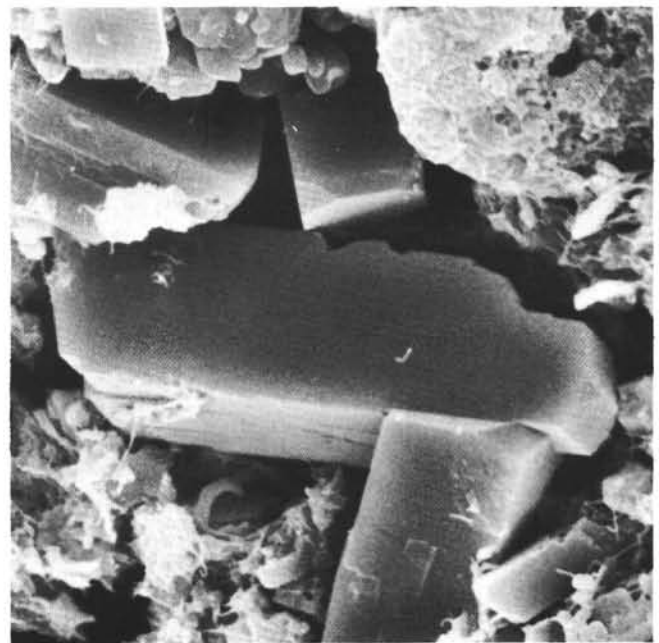
250 μm



30 μm



20 μm



10 μm

Plate 1. 1. Large plagioclase phenocryst in altered basaltic glass matrix, plagioclase partially replaced by analcime, Phase 1 volcanism, Sample 553A-36-2, 46-48 cm, transmitted light. 2. Authigenic smectite rimming altered pyroclasts, Phase 2 volcanism, Sample 555-41-1, 40-42 cm, SEM. 3. Bladed authigenic celadonite in Phase 2 lapilli tuff; Sample 553A-12-5, 30-32 cm, SEM. 4. Euhedral clinoptilolite in nonvolcanogenic sediment, Sample 552-9-5, 36-38 cm, SEM.

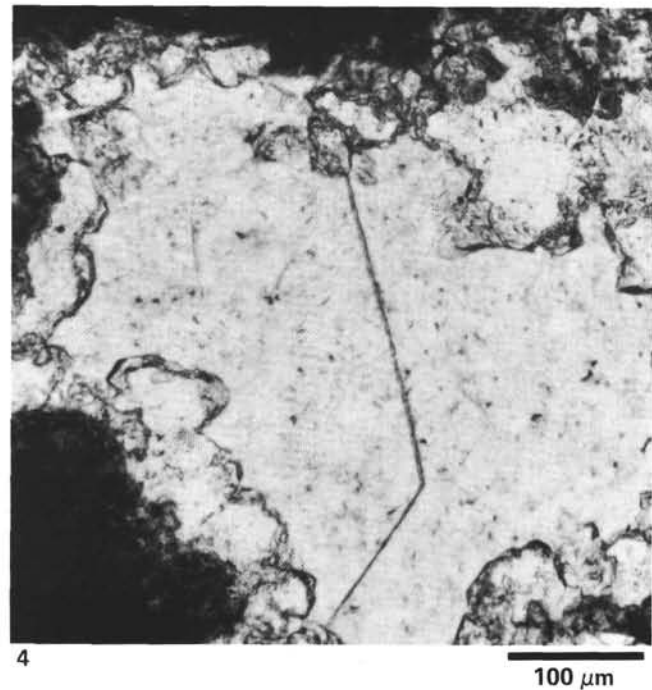
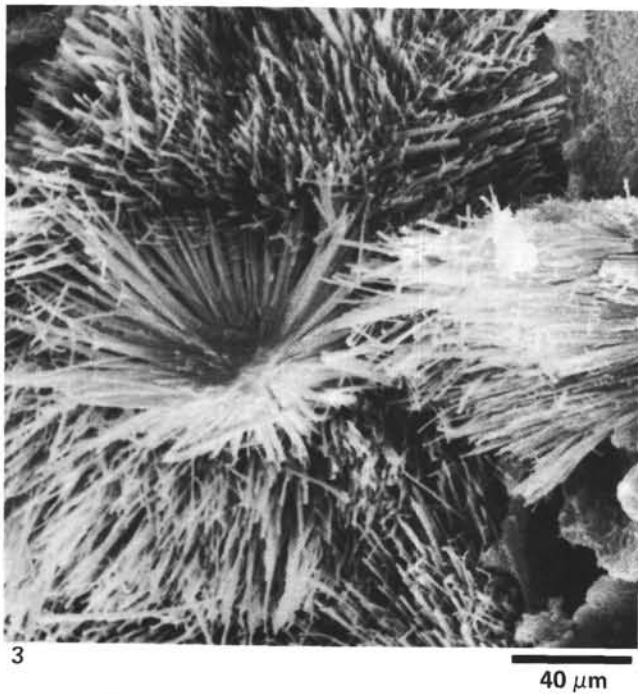
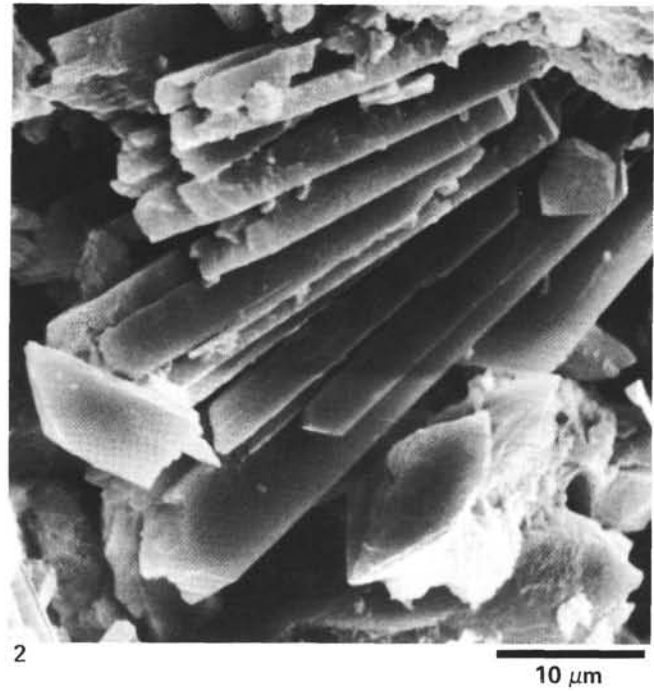
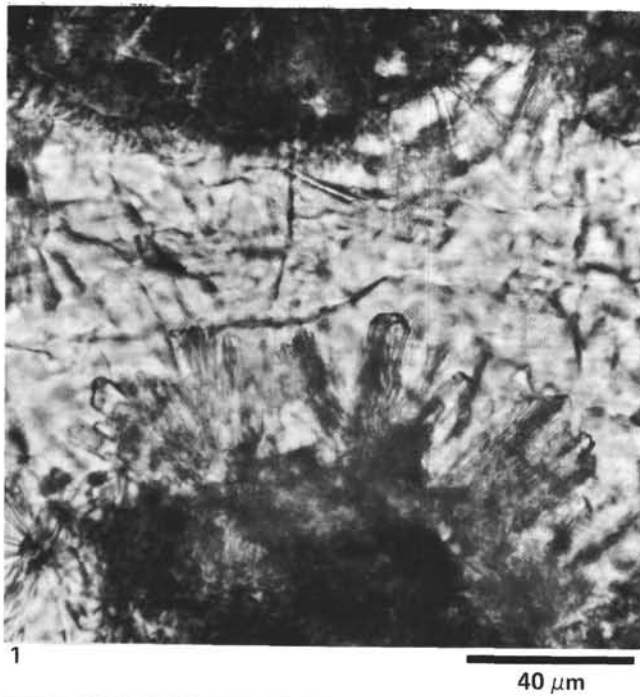


Plate 2. 1. Thin section photomicrograph of Phase 2 tuff with secondary radiating phillipsite and subsequent pore-filling calcite, Sample 555-46-2, 66-70 cm. 2. Radiating phillipsite as shown by SEM, Phase 2 volcanism, Sample 553A-19-2, 90-91 cm. 3. Fibrous zeolite (mordenite) in Phase 3 tuff, Sample 552-19, CC, SEM. 4. Thin section photomicrograph of Phase 1 lapilli tuff showing secondary analcime enclosed by later sparry calcite (compare Fig. 1); Sample 555-67-4, 120-122 cm.